gesting that the receptors mediating these opposing responses are different. The present study unequivocally demonstrates the existence of a subtype of receptor that is nonselective among endothelin isopeptides. This pharmacological property is indeed different from that observed in the receptor(s) on vascular smooth muscle cells[22] and several other types of cells[23–26], which to detect mRNA for the present endothelin receptor in vascular smooth muscle cells either *in vivo* or in culture. Receptors which do not distinguish between ET-1 and ET-3 have been identified pharmacologically in several cell types[27,28]. Rat osteosarcoma ROS 17/2 cells, which respond equally to ET-1 and ET-3 with a transient increase of $[Ca^{2+}]_i$ (data not shown), express the present endothelin receptor mRNA in abundance (Fig. 3).

We propose that the non-isopeptide-selective endothelin receptor described in this study be called the ET_B endothelin receptor, whereas the ET-1/ET-2-selective subtype in, for example, vascular smooth muscle cells be called the ET_A receptor. Cloning of the ET_A receptor will enable us to understand better the mechanisms for the diverse physiological roles of the endothelin family. □

Received 10 October; accepted 15 November 1990.

1. Yanagisawa, M. *et al. Nature* **332,** 411–415 (1988).
2. Yanagisawa, M. & Masaki, T. *Trends pharmacol. Sci.* **10,** 374–378 (1989).
3. Inoue, A. *et al. proc. natn. Acad. Sci. U.S.A.* **86,** 2863–2867 (1989).
4. Masuda, Y. *et al. FEBS Lett.* **257,** 208–210 (1989).
5. Kloog, Y., Bousso, M. D., Bdolah, A. & Sokolovski, M. *FEBS Lett.* **253,** 199–202 (1989).
6. Maggi, C. A. *et al. Eur. J. Pharmac.* **176,** 1–9 (1990).
7. Warner, T. D., de Nucci, G. & Vane, J. R. *Eur. J. Pharmac.* **159,** 325–326 (1989).
8. Kasuya, Y. *et al. Biochem. biophys. Res. Commun.* **61,** 1049–1055 (1989).
9. Takuwa, Y. *et al. J. clin. Invest.* **85,** 653–658 (1990).
10. Resink, T. J., Scott-Burden, T. & Buhler, F. R. *Eur. J. Biochem.* **189,** 415–421 (1990).
11. Seed, B. *Nature* **329,** 840–842 (1987).
12. Koseki, C., Imai, M., Hirata, Y., Yanagisawa, M. & Masaki, T. *Am. J. Physiol.* **256,** R858–R866 (1989).
13. MacCumber, M. W., Ross, C. A., Glaser, B. M. & Snyder, S. H. *Proc. natn. Acad. Sci. U.S.A.* **86,** 7285–7289 (1989).
14. Shaw, G. & Kamen, R. *Cell* **46,** 659–667 (1986).
15. von Heijine, G. *Nucleic Acids Res.* **14,** 4683–4690 (1989).
16. Schvartz, I., Ittoop, O. & Hazum, E. *Endocrinology* **126,** 3218–3222 (1990).
17. Strader, C. D., Irving, S. S. & Richard, A. F. *FASEB J.* **3,** 1825–1832 (1989).
18. Permentier, M. *et al. Science* **246,** 1620–1622 (1989).
19. McFarland, C. *et al. Science* **245,** 494–499 (1989).
20. Kobilka, B. *et al. Science* **240,** 1310–1316 (1988).
21. Fukuda, N. *et al. Biochem. biophys. Res. Commun.* **167,** 739–745 (1990).
22. Hirata, Y. *et al. Biomed. Res.* **11,** 195–198 (1990).
23. Takuwa, Y., Masaki, T. & Yamashita, K. *Biochem. biophys. Res. Commun.* **170,** 998–1005 (1990).
24. Bousso, M. D. *et al. Biochem. biophys. Res. Commun.* **162,** 952–957 (1989).
25. Ohnishi-Suzaki, A. *et al. Biochem. biophys. Res. Commun.* **166,** 608–614 (1990).
26. Cozza, E. N., Gomez-Sanchez, C. E., Foecking, M. F. & Chiou, S. *J. clin. Invest.* **84,** 1032–1035 (1989).
27. Marsault. R., Vigne, P., Breittmayer, J. P. & Frelin, C. *J. Neurochem.* **54,** 2142–2144 (1990).
28. Martin, E. R., Brenner, B. M. & Ballermann, B. *J. biol. Chem.* **265,** 14044–14049 (1990).
29. Sambrook, J., Fritsch, E. F. & Maniatis, T. *Molecular Cloning: A Laboratory Manual* (Cold Spring Harbor Laboratory, New York, 1989).
30. Kozak, M. *Nucleic Acids Res.* **12,** 857–874 (1984).

ACKNOWLEDGEMENTS. We thank H. Nakauchi for discussion. This work was supported in part by the Ministry of Education, Science and Culture of Japan, the Uehara memorial Foundation, Toray Scientific foundation and the University of Tsukuba Project Research.

Cytosolic Ca^{2+} gradients triggering unidirectional fluid secretion from exocrine pancreas

Haruo Kasai* & George J. Augustine*

Max-Planck-Institut für biophysikalische Chemie, am Fassberg, D-3400, Göttingen, Germany

EXOCRINE gland cells secrete Cl^--rich fluid when stimulated by neurotransmitters or hormones[1]. This is generally ascribed to a rise in cytosolic Ca^{2+} concentration[2] ($[Ca^{2+}]_i$), which leads to activation of Ca^{2+}-dependent ion channels[3,4]. A precise understanding of Cl^- secretion from these cells has been hampered by a lack of knowledge about the spatial distribution of the Ca^{2+} signal and of the Ca^{2+}-dependent ion channels in the secreting epithelial cells[4]. We have now used the whole-cell patch-clamp method and digital imaging[5] of $[Ca^{2+}]_i$ to examine the response of rat pancreatic acinar cells to acetylcholine. We found a polarization of $[Ca^{2+}]_i$ elevation and ion channel activation, and suggest that this comprises a novel 'push–pull' mechanism for unidirectional Cl^- secretion. This mechanism would represent a role for cytosolic Ca^{2+} gradients in cellular function. The cytosolic $[Ca^{2+}]_i$ gradients and oscillations of many other cells[2] could have similar roles.

Single acinar cells responded to acetylcholine (ACh) with a rise in $[Ca^{2+}]_i$ (Fig. 1)[6–8], which was mainly due to release of Ca^{2+} from internal stores[9], because its amplitude was not altered by the removal of external Ca^{2+} (data not shown). Exposure to ACh also elicited an ionic current carried by Cl^--permeable channels and an ionic current through cation-permeable channels[10,11]. These currents were activated by an ACh-induced rise in $[Ca^{2+}]_i$ (refs 10–12), because they were eliminated by including the Ca^{2+} buffer, EGTA (data not shown).

The Cl^- current had two transient components ($n = 13$) at 0 mV, the reversal potential of the cation current[10,11]. An early component appeared abruptly, reached a peak within 0.5 s and then rapidly decayed (Fig. 1*a–c*); it occurred while there was little or no change in average $[Ca^{2+}]_i$ (Fig. 1*a–c*). The peak of the early component preceded the peak of the average $[Ca^{2+}]_i$ change by 1.5–8 s (mean 2.6 s, $n = 13$; Fig. 1). The early component was usually followed by a longer-lasting component (Fig. 1*a*, *b*), the peak amplitude and time of appearance of which were more variable than those of the early component (Fig. 1*b*). Both the time course and amplitude of the late component paralleled those of the average $[Ca^{2+}]_i$ signal (Fig. 1*a–c*). A similar biphasic Cl^- current occurs in the lacrimal gland[13].

Current flowing through the cation-permeable channels, measured at −40 mV, the reversal potential of the Cl^- currents (E_{Cl})[10,11], was monophasic (Fig. 1*d*, middle trace; $n = 8$). The time course of the cation current correlated well with that of the rise in average $[Ca^{2+}]_i$ (Fig. 1*d*, lower trace). Thus, ACh first activates an early Cl^- current, which is followed by the simultaneous appearance of a cation current, a late Cl^- current and a rise in average $[Ca^{2+}]_i$ (Fig. 1*d*, upper trace).

That the early Cl^- current rises before the change in average $[Ca^{2+}]_i$ suggests spatial heterogeneity of the $[Ca^{2+}]_i$ signal[8,14]. Digital imaging was used to determine whether spatial gradients in the $[Ca^{2+}]_i$ signal could explain this temporal discrepancy. In every cell examined ($n = 18$), ACh initially increased $[Ca^{2+}]_i$ at the edge of the luminal pole of the acinar cell and the $[Ca^{2+}]_i$ rise then slowly spread towards the basal pole (Fig. 2*b–h*). The same pattern of $[Ca^{2+}]_i$ rise was detected during Ca^{2+} oscillations induced by a lower concentration of ACh (0.33 μM, data not shown). This pattern is surprising because the muscarinic receptors for ACh are thought to be localized to the basolateral membrane[3,4]. This suggests that there is either positioning of ACh receptors close to the luminal membrane or luminal localization of specific Ca^{2+}-releasing organelles, highly sensitive to ACh stimulation, that have yet to be identified[15,16].

The spatial pattern of the ACh-induced Ca^{2+} signal is shown graphically in Fig. 3. The $[Ca^{2+}]_i$ signal was initially greatest at the luminal end and sharply declined in the basolateral direction, suggesting that Ca^{2+} release initially occurs just beneath the luminal plasma membrane. After the initial luminal rise in $[Ca^{2+}]_i$, a wave of elevated $[Ca^{2+}]_i$ spread towards the basolateral side and travelled at about 10 μm s^{-1} (range 6–25 μm s^{-1}, $n = 6$; ref. 2). During this Ca^{2+} wave, $[Ca^{2+}]_i$ continued to rise

* Present addresses: Department of Physiology, Faculty of Medicine, University of Tokyo, Hongo 7-3-1, Bunkyo-ku, Tokyo, 113 Japan (H.K.) and Section of Neurobiology, Department of Biological Sciences, University of Southern California, Los Angeles, California 90089-2520, USA (G.J.A.).

throughout the cell, usually reaching its maximal value at the basal pole (Fig. 3*b*, *c*). The spatial distribution of this secondary rise implies two different Ca^{2+} release mechanisms: a release from a store in the luminal side that is sensitive to inositol trisphosphate[2]; and a Ca^{2+}-activated Ca^{2+} release[13] in the basolateral side. For comparison with the measurements of average $[Ca^{2+}]_i$ changes recorded during the patch-clamp experiments, a spatially averaged $[Ca^{2+}]_i$ signal was calculated from the imaging data (Fig. 3*c*, solid line). This signal lagged behind the luminal $[Ca^{2+}]_i$ changes by 0.1–0.9 s ($n = 5$). The initial luminal $[Ca^{2+}]_i$ rise was largely absent from the average $[Ca^{2+}]_i$ signal because of the small relative volume of the luminal pole.

The spatio-temporal features of the Ca^{2+} signal allows interpretation of the pattern of activation of Ca^{2+}-dependent currents. The early Cl^- current is temporally correlated with the early spatially restricted increase in $[Ca^{2+}]_i$ at the luminal pole and, therefore, must flow through Cl^-channels in the luminal membrane. The peak amplitude of the early Cl^- current is always larger than that of the late Cl^- current (Fig. 1*a*–*c*), even though the relevant $[Ca^{2+}]_i$ levels and membrane areas are smaller at the luminal pole, suggesting that the Cl^- channels there are present at a high density and closely associated with Ca^{2+}-release sites. The transient nature of the early Cl^- current could be caused by closure of the channel despite a sustained rise in luminal $[Ca^{2+}]_i$ (Fig. 3*c*) or could result from a highly localized decline in $[Ca^{2+}]_i$ that is beyond the spatial resolution of our measurements (~2 μm). The late Cl^- current and the cation current could flow through the basolateral regions, because their activation most closely parallels the slower $[Ca^{2+}]_i$ changes in the bulk of the cell. This is consistent with previous findings that Cl^- (ref. 17) and cation[18] conductances in the basolateral membrane of various exocrine cells are increased by ACh.

This pattern of channel activation suggests a 'push–pull' model for unidirectional Cl^- transport across the acinus (Fig. 4). In this model, secretagogues shift the acinar cell from a resting phase to a 'push' phase during which only the luminal Cl^- channels are activated. This will yield a secretion (or pushing) of Cl^- into the lumen because the membrane potential, V_m, is more negative than E_{Cl} (Fig. 4 legend). As the Ca^{2+} signal spreads, the 'pull' phase will occur because of the activation of the cation channel, which depolarizes V_m and reverses the electrochemical gradient for Cl^-. Chloride is then pulled into the acinus by influx through basolateral Cl^- channels. Given these fluxes of Cl^-, Na^+ may then flow through paracellular

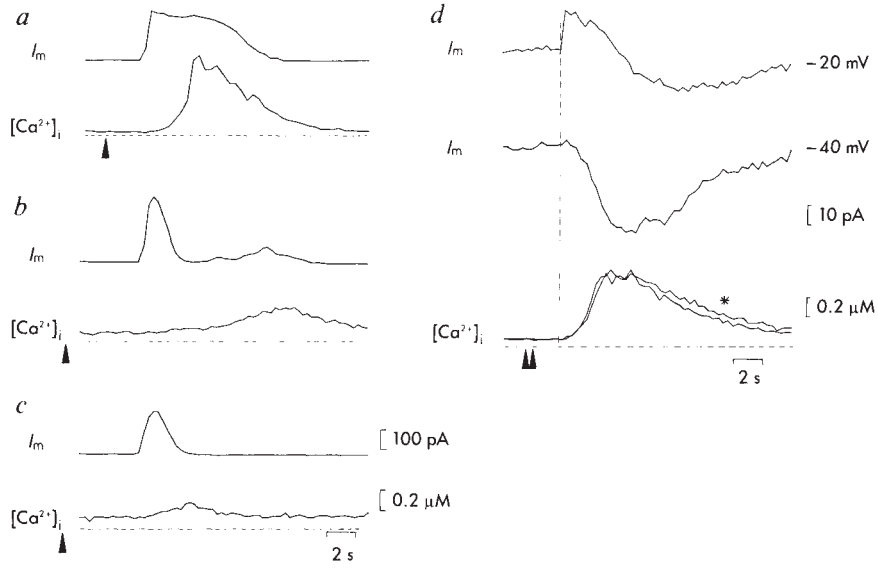

FIG. 1 Average $[Ca^{2+}]_i$ and current responses to ACh (10 μM) recorded from single rat pancreatic acinar cells with combined Fura-2 and patch clamp measurements; *a*–*d* were recorded from four different cells. *a*–*c*, Membrane potential was held at 0 mV. ACh application was begun at times indicated by the arrowheads. *d*, Responses to two applications of ACh were measured at two different potentials (−20 and −40 mV); current traces are aligned to superimpose the $[Ca^{2+}]_i$ traces. Asterisk and left arrowhead refer to recordings made while the cell was held at −20 mV. Horizontal dotted lines indicate $[Ca^{2+}]_i$ of 0 μM. A vertical dotted line in *d* shows the onset of the Cl^- current. Similar patterns of current activation and $[Ca^{2+}]_i$ rise were also seen with 1 μM and 0.5 μM ACh.

METHODS. Cells were dissociated from pancreatic acini of 3–6-week-old Wistar rats, using collagenase and trypsin[10]. A recording chamber was superfused with a solution containing: 140 mM NaCl, 2.8 mM KCl, 2 mM $MgCl_2$, 1 mM $CaCl_2$, 11 mM glucose and 10 mM NaHEPES at pH 7.2. Patch pipettes (4–6 MΩ) were filled with a solution containing: 135 mM potassium glutamate, 20 mM NaCl, 1 mM $MgCl_2$, 0.2 mM Na_2-ATP, 0.1 Fura-2 pentapotassium salt (Molecular Probes) and 10 mM Na-HEPES at pH 7.2. All measurements of potential were corrected for a junction potential between the pipette and bathing solution of −8 mV. Series resistance between the cells and pipettes ranged from 8 to 15 MΩ. Voltage clamp experiments were made using an EPC-9 amplifier (HEKA Electronics). The methods used for measuring average $[Ca^{2+}]_i$ with a photomultiplier have been described[23]. All experiments were at room temperature (23–26 °C).

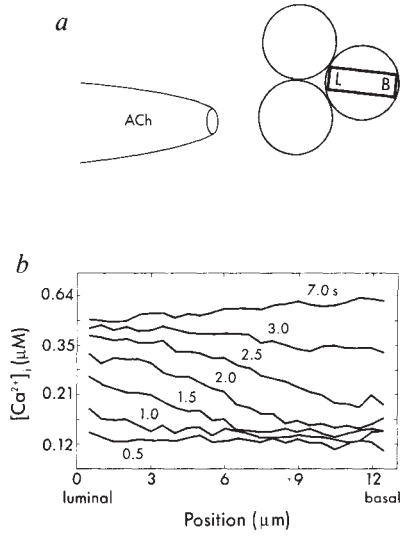

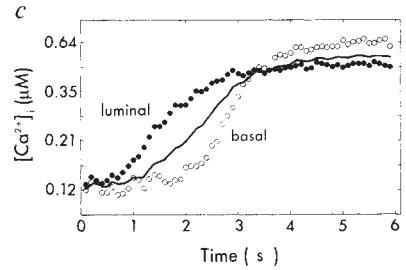

FIG. 3 Spatial and temporal features of ACh-induced $[Ca^{2+}]_i$ changes. *a*, Schematic diagram of the cell cluster shown in Fig. 2, indicating the scanning areas analysed in *b* and *c*. *b*, Spatial profile of $[Ca^{2+}]_i$ changes was scanned along the luminal–basal axis of the indicated cell. *c*, The time course of $[Ca^{2+}]_i$ changes caused by ACh were measured in 1-μm-wide areas at the two extreme poles of the cell (B and L in Fig. 3*a*). Solid line indicates the average change calculated by integrating over the entire area shown in *a*. Similar patterns were observed in all 18 cells tested, including three solitary cells not attached to a cluster. All cells within a cluster (or elsewhere within the field of ACh application) responded in this way, although the cells adjacent to the ACh-application pipettes invariably responded first (as in Fig. 2*b*).

pathways[1], because of the negativity of the lumen caused by the opening of luminal Cl^- channels[3]. Water flux will then osmotically follow these ion movements. Thus, the model proposes that the unidirectional secretion of iso-osmotic NaCl-rich fluid is directly caused by polarized activation of Ca^{2+}-dependent ion channels. Pumps and carriers[3,4] have an indirect role, that is in generating the electrochemical gradients used by the ion channels during secretion. The model could represent the first example of a cellular function that requires cytosolic Ca^{2+} gradients. Minor variations in this model would account for Ca^{2+}-dependent fluid secretion from other exocrine glands[1,3,4] (Fig. 4 legend).

The push–pull model circumvents previous difficulties in accounting for unidirectional fluid flow[3,4] despite a predicted influx of Cl^- from the lumen to the acinus when the cation channels and the luminal Cl^- channels are simultaneously opened. Several observations support predictions that arise from the model. First, reducing the driving force for the inward movement of Cl^- during the pull phase should prevent secretion. Indeed, reducing external Na^+ concentration prevents ACh-dependent depolarization and inhibits secretion[19]. Second, reducing the driving force for the outward movement of Cl^-

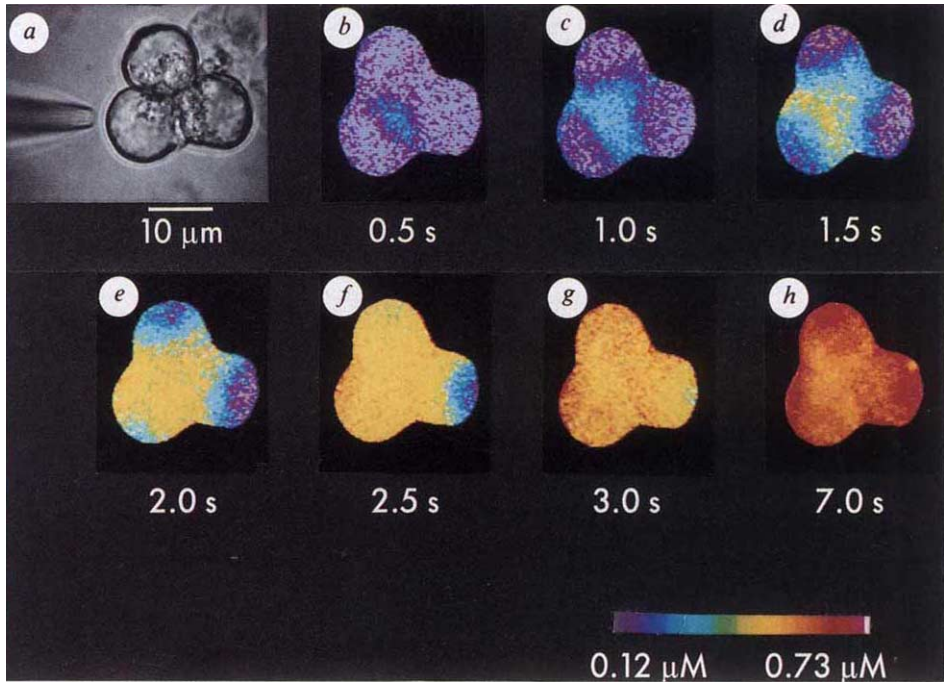

FIG. 2 Digital imaging of ACh-induced $[Ca^{2+}]_i$ changes in acinar cells. *a*, Bright-field micrograph of a cluster of three acinar cells. In the intact exocrine gland, part of the surface membrane of these cells (the luminal pole) is in contact with the lumen of the gland and the rest of it is in contact with the interstitial fluid (the basolateral membrane)[1]. Even after cell dissociation, the presence of visible zymogen granules makes it easy to identify the luminal pole of the pancreatic acinar cell[26]. Further, the attachments between cells within a triplet occurred at this pole. Thus, there was no ambiguity in defining cell orientation or the relative position of $[Ca^{2+}]_i$ changes within the cells. An application pipette containing 10 μM ACh is visible at the left of the cluster. *b–h*, Digital maps of changes in $[Ca^{2+}]_i$ induced by ACh. Timescale is relative to the earliest detectable response in the leftmost cell of the cluster. The changes in $[Ca^{2+}]_i$ were encoded with the pseudocolour scale shown at the bottom.

METHODS. Acinar cells were loaded with membrane-permeant Fura-2-AM, by incubating the cells with 3.3 μM Fura-2-AM for 30 min at 37 °C, and washed for 10 min at the same temperature. Details of the methods used for high time-resolution digital imaging of Ca^{2+} are described in detail elsewhere[24]. In brief, cells were excited with a single wavelength (390 nm, 10 nm bandpass) and the time-dependent changes in dye fluorescence were measured and digitally converted into a ratio by dividing by the fluorescence measured before agonist stimulation. As long as the path length and dye concentration are constant during the response, such a ratio yields a measure of relative $[Ca^{2+}]_i$ that is comparable to the more conventional two-excitation wavelength method[5]. This relative ratio can be converted to an absolute $[Ca^{2+}]_i$ level if the $[Ca^{2+}]_i$ before treatment is known (G.J.A. and E. Neher, manuscript in preparation). In our experiments, we assumed that the resting $[Ca^{2+}]_i$ was spatially uniform and was equivalent to 0.12 μM, the mean of 12 two-wavelength measurements made with a photomultiplier (Fig. 1 legend). Fluorescence images were obtained with a SIT camera (effective frequency response ~10 Hz) and stored at video rates (30 images s^{-1}) on an optical disc video recorder (Panasonic TQ-2026F). Individual images were then digitized offline, with a Matrox MVP-AT frame grabber board, to calculate the fura-2 fluorescence change ratios. (Kanno *et al.*[25] have reported lower-resolution (0.033 Hz) two-wavelength ratio images from pancreatic cells treated with cholecystokinin. They have also found that this agonist produces sustained rises in $[Ca^{2+}]_i$ in the basolateral pole of these cells, but their measurements were too slow to capture the early luminal signal we report here.)

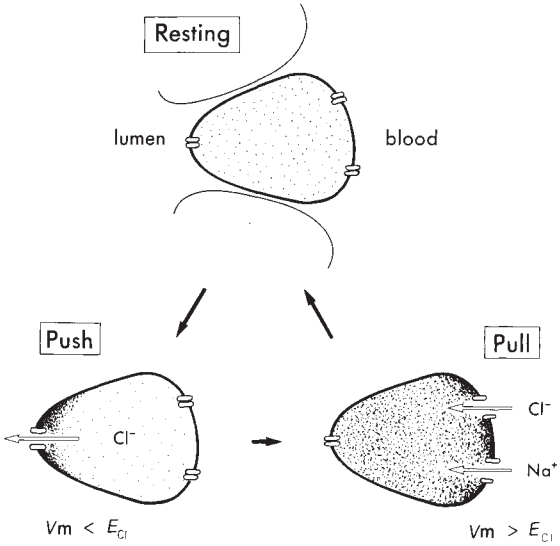

FIG. 4 A 'push–pull' model for Cl^- secretion in the rat pancreas. $[Ca^{2+}]_i$ is represented by the density of dotting. During a $[Ca^{2+}]_i$ rise induced by ACh, the acinus cycles through 'resting', 'push' and 'pull' phases. During the push phase, $[Ca^{2+}]_i$ selectively rises at the luminal pole of the cell and activates Cl^- channels. For Cl^- secretion into the lumen, V_m must be more negative than E_{Cl} at the luminal membrane. Microelectrode measurements in intact acini suggest that this is the case, because of a permeability of the resting cell to K^+ and active accumulation of Cl^- ($V_m = -39$ mV and $E_{Cl} = -33$ mV, ref. 1, assuming luminal fluid to be isotonic NaCl and isopotential to interstitial fluid). During the pull phase, the $[Ca^{2+}]_i$ increase spreads to the basolateral side to activate Cl^- and cation channels. For Cl^- uptake into the acinus, V_m must be more positive than E_{Cl} at the basolateral membrane. Measurements of the changes in V_m produced by ACh indicate that this is the case ($V_m = -20$ mV and $E_{Cl} = -33$ mV)[1]. Accumulation of internal Cl^- during the pull phase may also make E_{Cl} more positive and thereby enhance Cl^- secretion during the next push phase. The acinar cell may revert directly from the push phase to the resting phase, if a $[Ca^{2+}]_i$ rise is not sufficient to activate basolateral channels (as in Fig. 1*c*; see also Fig. 2 in ref. 8). Minor variations in this model also may account for Ca^{2+}-dependent fluid secretion from other exocrine glands[1,3,4]; for example, adding Ca^{2+}-activated K^+ channels[4,17] to the luminal pole could account for K^+ secretion from rat parotid gland.

during the push phase should prevent secretion; depolarization with high extracellular K^+ inhibits secretion[20]. Finally, oscillatory $[Ca^{2+}]_i$ changes should yield more secretion than a sustained rise in $[Ca^{2+}]_i$; maximal secretion occurs at a concentration of ACh (0.3 μM)[21] which produces oscillations in $[Ca^{2+}]_i$[8,9]. In blowfly salivary gland, secretion also increases with the frequency of V_m oscillations, presumably reflecting oscillatory $[Ca^{2+}]_i$ changes[22]. The generation and dissipation of localized $[Ca^{2+}]_i$ gradients may provide a rationale for the oscillatory $[Ca^{2+}]_i$ signalling of many cell types[2]. □

Received 9 August; accepted 12 October 1990.

1. Petersen, O. H. *The Electrophysiology of Gland Cells* (Academic, New York, 1980).
2. Berridge, M. J. & Irvine, R. F. *Nature* **341,** 197–205 (1989).
3. Petersen, O. H. & Gallacher, D. V. *A. Rev. Physiol.* **50,** 65–80 (1988).
4. Marty, A. *Trends Neurosci.* **10,** 373–377 (1987).
5. Tsien, R. Y. & Poenie, M. *Trends Biochem. Sci.* **11,** 450–455 (1988).
6. Merritt, J. E. & Rubin, R. P. *Biochem. J.* **230,** 151–159 (1985).
7. Bruzzone, R., Pozzan, T. & Wollheim, C. B. *Biochem. J.* **235,** 139–143 (1986).
8. Oscipchuk, Y. V., Wakui, M., Yule, D. I., Gallacher, D. V. & Petersen, O. H. *EMBO J.* **9,** 697–704 (1990).
9. Wakui, M., Potter, B. V. L. & Petersen, O. H. *Nature* **339,** 317–320 (1989).
10. Maruyama, Y. *J. Physiol.* **406,** 299–313 (1988).
11. Randriamampita, C., Chanson, M. & Trautmann, A. *Pflügers Arch.* **411,** 53–57 (1988).
12. Laugier, R. & Petersen, O. H. *Pflügers Arch.* **386,** 147–152 (1980).
13. Marty, A. & Tan, Y. P. *J. Physiol.* **419,** 665–687 (1989).
14. Foskett, J. K., Gunter-Smith, P. J., Melvin, J. E. & Turner, R. J. *Proc. natn. Acad. Sci. U.S.A.* **86,** 167–171 (1989).
15. Schulz, I., Thevenod, F. & Dehlinger-Kremer, M. *Cell Calcium* **10,** 325–336 (1989).
16. Volpe, P., Krause, K., Hashimoto, S., Zorzato, F., Pozzan, T., Meldolesi, J. & Lew, D. P. *Proc. natn. Acad. Sci. U.S.A.* **85,** 1091–1905 (1988).
17. Marty, A., Tan, Y. P. & Trautmann, A. *J. Physiol.* **357,** 293–325 (1984).
18. Maruyama, Y. & Petersen, O. H. *Nature* **299,** 159–161 (1982).
19. Petersen, O. H. & Ueda, N. *J. Physiol.* **264,** 819–835 (1977).
20. Petersen, O. H. *Experimentia* **26,** 1103–1104 (1970).
21. Habara, Y. *Jap. J. Physiol.* **30,** 561–574 (1980).
22. Rapp, P. E. & Berridge, M. J. *J. exp. Biol.* **93,** 119–132 (1981).
23. Neher, E. in *Neuromuscular Junction* (eds Sellin, L. C., Libelius, R. & Thesleff, S.) 65–76 (Elsevier, Amsterdam, 1989).
24. Smith, S. J., Osses, L. R. & Augustine, G. J. in *Calcium and Ion Channel Modulation,* (eds Grinnell, A. D., Armstrong, D. & Jackson, M. B.) 147–155 (Plenum, New York, 1988).
25. Kanno, T., Saito., T. & Yasmashita, T. *Biomed. Res.* **10,** 475–484 (1989).
26. Amsterdam, A. & Jamieson, J. D. *Proc. natn. Acad. Sci. U.S.A.* **69,** 3028–3032 (1972).

ACKNOWLEDGEMENTS. We thank E. Neher for support, facilities and naming the 'push-pull' model; and C. Augustine, M. Cahalan, R. Cahalan, D. Chien, S. Garber, F. von zur Mühlen, E. Neher and R. Penner for commenting on this paper. This work was supported by Alexander von Humboldt Fellowships, the NIH (G.J.A.) and a Leibniz award of the DFG (E.N.).

MHC class II region encoding proteins related to the multidrug resistance family of transmembrane transporters

Edward V. Deverson, Irene R. Gow, W. John Coadwell, John J. Monaco*, Geoffrey W. Butcher & Jonathan C. Howard

Department of Immunology, Institute of Animal Physiology and Genetics, Cambridge Research Station, Babraham Hall, Babraham, Cambridge CB2 4AT, UK
* Department of Microbiology and Immunology, Medical College of Virginia/Virginia Commonwealth University, Richmond, Virginia 23298-0678, USA

THE T-cell immune response is directed against antigenic peptide fragments generated in intracellular compartments, the cytosol or the endocytic system[1]. Peptides derived from cytosolic proteins, usually of biosynthetic origin, are presented efficiently to T-cell receptors by major histocompatibility complex (MHC) class I molecules[2–4], with which they assemble, probably in the endoplasmic reticulum (ER)[5]. In the absence of recognizable N-terminal signal sequences, such cytosolic peptides must be translocated across the ER membrane by a novel mechanism. Genes apparently involved in the normal assembly and transport of class I molecules may themselves be encoded in the MHC[6–8]. Here we show that one of these, the rat *cim* gene[6], maps to a highly polymorphic part of the MHC class II region encoding two novel members of the family of transmembrane transporters related to multidrug resistance[9,10]. Other members of this family of transporter proteins are known to be capable of transporting proteins[11,12] and peptides[13] across membranes independently of the classical secretory pathway. Such molecules are credible candidates for peptide pumps that move fragments of antigenic proteins from the cytosol into the ER[14,15].

The existence of a distinct peptide transporter for class I molecules was proposed initially to account for the properties of the mutant mouse cell line, RMA-S (ref. 5). Class I MHC molecules in RMA-S fail to assemble normally in the ER, and the cell is unable to present peptides of biosynthetic origin to T cells. The human cell line CEM.174 shows a similar phenotype, and in this case the lesion has been mapped to a large deletion in the MHC between DPA and the class III region[16] (Fig. 1*a*). Natural alleles at the rat *cim* locus modify the specificity of class I antigen presentation and the time of residence of newly synthesized class I molecules in the ER (ref. 6, and S. Powis *et al.*, manuscript submitted). It has therefore been suggested that the *cim* locus product may also be involved in peptide loading or assembly of class I histocompatibility antigens. The *cim* locus has been mapped into the rat MHC as *RT1* (Fig. 1*b*) between the presumed DP homologue, *RT1.H* (represented by Pb in *H-2,* Fig. 1*c*), and the DQA homologue, $RT1.B_\alpha$ (represented by Aa in *H-2*) (A. M. Livingstone *et al.*, manuscript submitted). The enclosed segment is included in, but smaller than, the HLA deletion in the CEM.174 cell line.

We looked for *cim* by screening a rat concanavalin-A lymphoblast complementary DNA library[17] using as probes inserts from an overlapping set of mouse cosmids covering the *cim* region[18] (Fig. 1*c*). Two relatively abundant cDNAs (about 1 in 10^4 clones) hybridizing with cosmids 5.10 and 508 were recovered. We propose the names *mtp1* and *mtp2* (for MHC-linked transporter protein) for the rat genes (homologous mouse cDNAs have recently been isolated, and the mouse genes named *HAM1* and *HAM2*[19]). The rat *mtp* genes were distantly related to each other because their cDNAs cross-hybridized weakly. The two genes were mapped into the known restriction maps of the mouse cosmids[18] using rat cDNAs as probes (Fig. 1*d*). The mouse genes map 7 kilobases (kb) apart, about 14 kb centromeric to the Ob (formerly $A_{\beta 2}$) gene. A search for rat cosmids containing the *mtp* region was unsuccessful; cloning difficulties in the homologous region in the rat MHC have been noted before[20]. Accordingly, the rat *mtp* genes were mapped by restriction fragment length polymorphisms in Southern blots of genomic DNA from MHC congenic and recombinant rat strains (Fig. 2). Both genes mapped into the same region of the MHC as the *cim* gene. The genomic environments of both genes were notably polymorphic; three of the four genomic *Bam*H1 fragments of the *mtp1* gene showed allelic variation among the five haplotypes tested (Fig. 2*a*) as did the *Eco*R1 fragments of *mtp1.* The genomic blots showed no evidence for a family of close relatives.

The sequence of one putatively full-length *mtp1* cDNA clone, 510-15, is shown in Fig. 3. The 2,674-base-pair (bp) insert contains a single long open reading frame that is predicted to encode a polypeptide of 725 amino acids and to have a relative molecular mass of 79,000. The N terminus of the protein is conjectural, however spleen *mtp1* mRNA was indistinguishable in size by northern analysis from a T7 transcript of the 510-15 cDNA insert (data not shown). The mtp1 polypeptide showed a highly significant sequence similarity to the ATP-dependent transmembrane transporter proteins of the multidrug resistance (mdr) group[9], including both mammalian (mdr[21], CFTR[22]), yeast (STE6[13]) and prokaryotic (HlyB[11,12]) members (Fig. 4*a*). Proteins of this family are active transporters for a wide range of substances including long polypeptides[11,12], oligopeptides[13] and small hydrophobic compounds such as antibiotics and possibly steroids[23]. The family displays a conservative cytosolic